J Electr Eng Technol.2018; 13(1): 089-096
http://doi.org/10.5370/JEET.2018.13.1.089

ISSN(Print) 1975-0102
ISSN(Online) 2093-7423

An Improved Analytic Model for Power System Fault Diagnosis and its Optimal Solution Calculation

Shoupeng Wang† and Dongmei Zhao*

Abstract – When a fault occurs in a power system, the existing analytic models for the power system fault diagnosis could generate multiple solutions under the condition of one or more protective relays (PRs) and/or circuit breakers (CBs) malfunctioning, and/or an alarm or alarms of these PRs and/or CBs failing. Therefore, this paper presents an improved analytic model addressing the above problem. It takes into account the interaction between the uncertainty involved with PR operation and CB tripping and the uncertainty of the alarm reception, which makes the analytic model more reasonable. In addition, the existing analytic models apply the penalty function method to deal with constraints, which is influenced by the artificial setting of the penalty factor. In order to avoid the penalty factor's effects, this paper transforms constraints into an objective function, and then puts forward an improved immune clonal multi-objective optimization algorithm to solve the optimal solution. Finally, the cases of the power system fault diagnosis are served for demonstrating the feasibility and efficiency of the proposed model and method.

Keywords: Power system, Fault diagnosis, Analytic model, Multi-objective optimization, Immune memory

1. Introduction

As an important application to realize the self-healing ability of smart grids, the power system fault diagnosis plays a significant role in post-fault analysis and power supply restoration [1-2]. Therefore, several methods for the power system fault diagnosis using information from protective relays (PRs) and circuit breakers (CBs) have been proposed since 1970s [3], such as the methods based on artificial neural network [4], expert system [5], Petri net [6], Bayesian network [7], rough sets [8] and analytic model [9-14]. Especially, the analytic model-based method has the theoretical and mathematical foundation strictly. It can simplify logical inference and make software development easier. Therefore, this method has a promising prospect in engineering.

The analytic model-based methods build up an objective function which can reflect the relationship between the states of suspected fault components and the operating states of PRs and CBs. Then the power system fault diagnosis problem can be formulated as a 0-1 integer programming problem, and the optimization algorithm is used to solve the problem (i.e., to search for the most likely fault hypothesis (FH) that can well describe the realistic fault scenario) [14].

The analytic model-based methods are proposed in [10-14]. In [10-11], the objective function reflecting the discrepancy between the expected and the actual states of PRs and CBs is established, and Genetic Algorithm and Simulated Annealing are employed to find a FH which minimizes the defined objective function. The possibility of PRs' and CBs' malfunctions isn't considered in estimating the expected states of PRs and CBs, thus this model in [10-11] may lead to false diagnosis results. Based on [10-11], the analytic model in [12] takes into account malfunctions of PRs and CBs. The states of malfunctions are expressed as logical variables, and Tabu Search is employed to solve the model. This model can not only diagnose the fault component(s) accurately, but also identify the malfunctioned PRs and/or CBs. However, the received alarms of PRs and CBs are used to represent their actual states, and this model in [12] does not consider the failures of alarms. On the basis of [12], a complete analytic model in [13-14] is presented. The actual states of suspected fault components, the actual states of PRs and CBs as well as the malfunction states of PRs and CBs are regarded as logical variables in [13-14], which raises the anti-jamming capability of the analytic model. However, the complete analytic model does not consider the relationship between the malfunction event of PRs and CBs and the failure event of alarms, therefore it could have multiple solutions when more malfunctions of PRs and CBs and/or failures of alarms occur.

Base on the work presented in [13-14], an improved analytic model is developed for the power system fault diagnosis. It takes into account the interaction between the uncertainty involved with PR operation and CB tripping

† Corresponding Author: School of Electrical and Electronic Engineering, North China Electric Power University, Beijing, China. (wsp_ep@yahoo.com)
* School of Electrical and Electronic Engineering, North China Electric Power University, Beijing, China. (zhao-dm@ncepu.edu.cn)
Received: May 4, 2017; Accepted: August 21, 2017

and the uncertainty of the alarm reception, which makes the analytic model more reasonable. In addition, the constrained problem is solved with the penalty function method in the existing analytic models, which is influenced by the artificial setting of the penalty factor. In order to avoid the penalty factor's effects, this paper transforms constraints into an objective function, which converts the constrained optimization problem to the unconstrained multi-objective optimization problem. And an improved immune clonal multi-objective optimization algorithm can then be put forward to solve the problem. Finally, the cases of the power system fault diagnosis are applied to verify the feasibility and efficiency of the improved model and method.

2. Improved Analytic Model

When a fault occurs in a power system, the malfunction event of PRs and CBs and the failure event of alarms are related. For instance, when an alarm obtained from the console in the power dispatching center is incorrect, it can be explained as two cases: the incorrect alarm is the event of a PR operating or a CB being tripped incorrectly; the incorrect alarm is an incorrect alarm event and the rest of pertinent alarms do not exist. Therefore, this paper, on the basis of [13-14], presents an improved objective function which completely describes the relationships among the actual and the expected states of PRs and CBs and the received alarms. The improved objective function can be expressed as,

$$\begin{aligned} & E(\boldsymbol{G}) = \omega_1 E_1 + \omega_2 E_2 = \\ & \omega_1 \left[\sum_{i=1}^{n_r} \left| r_i(\boldsymbol{G}) - r_i^*(\boldsymbol{G}) \right| + \sum_{j=1}^{n_c} \left| c_j(\boldsymbol{G}) - c_j^*(\boldsymbol{G}) \right| \right] + \\ & \omega_2 \left[\sum_{i=1}^{n_r} \left| r_i' - r_i(\boldsymbol{G}) \right| + \sum_{j=1}^{n_c} \left| c_j' - c_j(\boldsymbol{G}) \right| \right] \\ & s.t.: \ \boldsymbol{h}(\boldsymbol{G}) \end{aligned} \tag{1}$$

where,

- $\boldsymbol{G}=(\boldsymbol{D}, \boldsymbol{R}, \boldsymbol{C}, \boldsymbol{F}, \boldsymbol{M})$ is a fault hypothesis (FH).
- $\boldsymbol{D}=(d_1, d_2, ..., d_i, ..., d_{n_d})$ is the set of suspected fault components in the outage area, and d_i represents the state of the i^{th} component, with d_i = 0 and 1, respectively, corresponding to its normal and fault states.
- $\boldsymbol{R}=(r_1, r_2, ..., r_i, ..., r_{n_r})$ is the set of PRs associated with $\boldsymbol{D}$, and r_i represents the state of the i^{th} PR, with r_i = 0 and 1, respectively, corresponding to its non-operational and operational states.
- $\boldsymbol{C}=(c_1, c_2, ..., c_i, ..., c_{n_c})$ is the set of CBs associated with $\boldsymbol{D}$, and c_i represents the state of the i^{th} CB, with c_i = 0 and 1, respectively, corresponding to its non-tripped (closed) and tripped (open) states.
- $\boldsymbol{M}=(m_{r_1}, m_{r_2}, ..., m_{r_{n_r}}, m_{c_1}, m_{c_2}, ..., m_{c_{n_c}})$. If r_i operates incorrectly, then m_{r_i} =1, otherwise m_{r_i} =0.
  In like manner, if c_i is tripped off incorrectly, then m_{c_i} =1, otherwise m_{c_i} =0.
- $\boldsymbol{F}=(f_{r_1}, f_{r_2}, ..., f_{r_{n_r}}, f_{c_1}, f_{c_2}, ..., f_{c_{n_c}})$. If r_i fails to operate, then f_{r_i} =1, otherwise f_{r_i} =0.
  In like manner, if c_i fails to be tripped off, then f_{c_i} =1, otherwise f_{c_i} =0.
- $r_i(\boldsymbol{G})$, $c_j(\boldsymbol{G})$ and $r_i^*(\boldsymbol{G})$, $c_j^*(\boldsymbol{G})$ indicate the functions of $\boldsymbol{G}$. $r_i(\boldsymbol{G})$ and $c_j(\boldsymbol{G})$ indicate the actual states of PRs and CBs; $r_i^*(\boldsymbol{G})$ and $c_j^*(\boldsymbol{G})$ indicate the expected states of PRs and CBs. r_i' and c_j' indicate the observed states of PRs and CBs (i.e., the received alarms of PRs and CBs).
- E_1 denotes the difference between the actual and the expected states of PRs and CBs, which reflects the malfunctions of PRs and CBs. ω_1 is the weight of E_1.
- E_2 denotes the difference between the observed and the actual states of PRs and CBs, which reflects the missing and incorrect alarms of PRs and CBs. ω_2 is the weight of E_2.
- $\boldsymbol{h}(\boldsymbol{G})$ = ($h(\boldsymbol{G})_{r_1}$, $h(\boldsymbol{G})_{r_2}$, ..., $h(\boldsymbol{G})_{r_{n_r}}$, $h(\boldsymbol{G})_{c_1}$, $h(\boldsymbol{G})_{c_2}$, ..., $h(\boldsymbol{G})_{c_{n_c}}$) indicates the operating logical constraints. $h(\boldsymbol{G})_{r_i}$ represents the logical constraint of the i^{th} PR. If $h(\boldsymbol{G})_{r_i}$ satisfies constraints, then $h(\boldsymbol{G})_{r_i}$ =0, otherwise $h(\boldsymbol{G})_{r_i}$ =1. The contradictory constraints of PR (i.e., $h(\boldsymbol{G})_{r_i}$ =1) include r_i =1 and f_{r_i} =1, r_i =0 and m_{r_i} =1, f_{r_i} =1 and m_{r_i} =1, r_i^* =0 and f_{r_i} =1, and r_i^* =1 and m_{r_i} =1.
  Similarly, $h(\boldsymbol{G})_{c_j}$ represents the logical constraint of the j^{th} CB. If $h(\boldsymbol{G})_{c_j}$ satisfies constraints, then $h(\boldsymbol{G})_{c_j}$ =0, otherwise $h(\boldsymbol{G})_{c_j}$ =1. The contradictory constraints of CB (i.e., $h(\boldsymbol{G})_{c_j}$ =1) include c_i =1 and f_{c_i} =1, c_i =0 and m_{c_i} =1, f_{c_i} =1 and m_{c_i} =1, c_i^* =0 and f_{c_i} =1, and c_i^* =1 and m_{c_i} =1.

The calculation method of the actual and the expected states and the values of the weights are specified in [13-14]. The objective function $E(\boldsymbol{G})$ completely describes the uncertainty about the PR operation, the CB tripping and the alarm reception, which reflects the credibility of $\boldsymbol{G}$.

In order to facilitate the following description, d_i, r_i, c_i, f_{r_i}, f_{c_i}, m_{r_i} and m_{c_i} represent not only their states but also their corresponding objects, and suffix i can be omitted without prejudice to comprehension.

3. Calculation and Analysis of Improved Analytic Model

The analytic model for the power system fault diagnosis employs the objection function $E(\boldsymbol{G})$ to express the logical relationships between the states of electrical components and the operating states of PRs and CBs, and applies the value of $E(\boldsymbol{G})$ to verify the credibility of FHs. Therefore, the power system fault diagnosis problem can be transformed into searching for a FH which minimizes

$E(\boldsymbol{G})$ with the constraints satisfied.

The expected, the actual, and the observed states of PRs and CBs associated with $\boldsymbol{D}$ are substituted into Eq. (1), and then $E(\boldsymbol{G})$ can be expressed as the function with $\boldsymbol{D}$, $\boldsymbol{R}$, $\boldsymbol{C}$, $\boldsymbol{F}$ and $\boldsymbol{M}$ as independent variables. The optimal solution ($\boldsymbol{D}^*$, $\boldsymbol{R}^*$, $\boldsymbol{C}^*$, $\boldsymbol{F}^*$, $\boldsymbol{M}^*$) can be obtained by using the optimization technique to minimize $E(\boldsymbol{G})$. $\boldsymbol{D}^*$ is applied to identify the real fault component; $\boldsymbol{F}^*$ and $\boldsymbol{M}^*$ are used to evaluate the operating states of PRs and CBs. Comparing $\boldsymbol{R}^*$ and $\boldsymbol{C}^*$ with their received alarms ($\boldsymbol{R}'$ and $\boldsymbol{C}'$), the evaluation results of the received alarms can be achieved. The evaluation equation is as follows,

$$\begin{cases} w_r = r'\overline{r} \\ l_r = \overline{r}'r \\ w_c = c'\overline{c} \\ l_c = \overline{c}'c \end{cases} \tag{2}$$

where,

- $r \in \boldsymbol{R}^*$ and $c \in \boldsymbol{C}^*$ indicate the actual states of PRs and CBs.
- $r' \in \boldsymbol{R}'$ and $c' \in \boldsymbol{C}'$ indicate the observed states of PRs and CBs.
- $w_r, w_c \in \boldsymbol{W}$; $\boldsymbol{W}$=($w_{r_1}, w_{r_2}, ..., w_{r_{n_r}}, w_{c_1}, w_{c_2}, ..., w_{c_{n_c}}$) is the set of incorrect alarms of PRs and CBs; if w_{r_i}=1, then the alarm corresponding to the i^{th} operational PR is incorrect, otherwise it is correct; if w_{c_i}=1, then the alarm corresponding to the i^{th} tripped CB is incorrect, otherwise it is correct.
- $l_r, l_c \in \boldsymbol{L}$; $\boldsymbol{L}$=($l_{r_1}, l_{r_2}, ..., l_{r_{n_r}}, l_{c_1}, l_{c_2}, ..., l_{c_{n_c}}$) is the set of the missing alarms of PRs and CBs; if l_{r_i}=1, then the alarm corresponding to the i^{th} operational PR is missing, otherwise it is not missing; if l_{c_i}=1, then the alarm corresponding to the i^{th} tripped CB is missing, otherwise it is not missing.

4. Basic Analysis of Improved Immune Clonal Multi-objective Optimization Algorithm and Its Application

4.1 Constraint processing method

The existing analytic models usually apply the penalty function method to deal with the constraint $\boldsymbol{h}(\boldsymbol{G})$ as shown in Eq. (1). Although the penalty function method is easy to perform, the artificial setting of the penalty factor is quite difficult. If the penalty factor is set too small, the calculated optimal solution may deviate from the true solution; if the penalty factor is set too large, the optimization algorithm has problem with the premature convergence [15]. Therefore, this paper transforms $\boldsymbol{h}(\boldsymbol{G})$ into an objective function in order to avoid the penalty factor's effects, which converts the constrained optimization problem to the unconstrained multi-objective optimization problem.

Converting the constraint in Eq. (1), Eq. (3) can be obtained as,

$$H_j(\boldsymbol{G}) = \left|h_j(\boldsymbol{G})\right|, \quad 1 \le j \le m \tag{3}$$

where, m is the number of logical constraint equations; $h_j(\boldsymbol{G})$ is the value of the j^{th} logical constraint equation. Transforming Eq. (3) into an objective function, Eq. (4) can then be obtained as,

$$H(\boldsymbol{G}) = \sum_{j=1}^{m} H_j(\boldsymbol{G}) \tag{4}$$

Therefore, the constrained optimization problem as shown in Eq. (1) is converted to an unconstrained multi-objective optimization problem, that is,

$$E'(\boldsymbol{G}) = \min\left(E(\boldsymbol{G}), H(\boldsymbol{G})\right) \tag{5}$$

Although Eq. (1) can be converted to Eq. (5), it is still different from the general multi-objective optimization problem. As for the general problem, the purpose of the calculation is to search for the best solutions with uniform distribution, which can well approach the Pareto front. As for Eq. (5), it is reverted to a single objective optimization problem in the feasible domain, where $H(\boldsymbol{G})$ = 0. In this way, the optimal solution of $E'(\boldsymbol{G})$ is the result of $E(\boldsymbol{G})$, so there is no need to consider about the distribution of Pareto optimal solutions.

4.2 Improved immune clonal multi-objective optimization algorithm

The immune clonal multi-objective optimization algorithm [16] regards the objective functions of the optimization problem as antigens of invading organism, and considers the feasible solutions corresponding to the objective functions as antibodies produced by the immune system. And the affinity is applied to explain the relationship between the antigen and the antibody, which describes the matching degree between the objective function and the feasible solution. Therefore, this paper employs the immune clonal multi-objective optimization algorithm to solve the power system fault diagnosis problem, and improves the algorithm via equipping with memory mechanism on the basis of [16]. The immune memory can promote the evolution of good individuals through elitism strategy, which enhances the global convergence of this method. The procedure of the improved algorithm is shown in Fig. 1. In Fig. 1, E^* denotes the optimal value of $E(\boldsymbol{G})$ corresponding to the optimal solution; E^{best} denotes the best value of $E(\boldsymbol{G})$ corresponding to the feasible solution in the current evolution algebra.

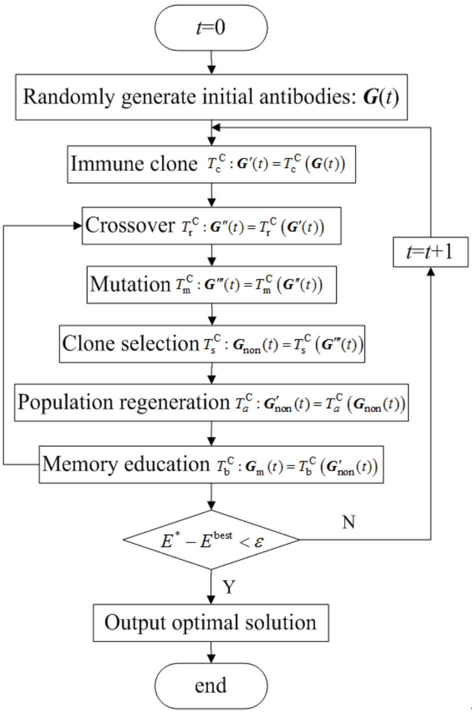

Fig. 1. Procedure of the improved immune clonal multi-objective optimization algorithm

The key operators in the procedure of the improved algorithm are as follows.

a) Immune clone operator $T_c^C : \boldsymbol{G}'(t) = T_c^C\left(\boldsymbol{G}(t)\right)$.

Employ the equal proportion clone method, and the equation of the clone is given by,

$$N_{ci} = \text{round}(\beta \times N) \tag{6}$$

where, N_{ci} indicates the clonal scale of the i^{th} antibody selected; β is propagation coefficient; N is the scale of the initial antibodies $\boldsymbol{G}(t)$. The scale of antibodies after cloning $\boldsymbol{G}(t)$ is given by,

$$N_c = \sum_{i=1}^{N} N_{ci} \tag{7}$$

b) Crossover operator $T_r^C : \boldsymbol{G}''(t) = T_r^C\left(\boldsymbol{G}'(t)\right)$.

Every antibody of $\boldsymbol{G}'(t)$ is performed crossover with probability p_c. For the binary encoding, the crossover operator mixes an antibody selected from $\boldsymbol{G}'(t)$ in the current evaluation algebra and another antibody selected from the memory cells $\boldsymbol{G}_m(t-1)$ in the previous evaluation algebra to generate a new antibody. The crossover operator is defined as follows,

$$\begin{aligned} G''_i(t) &= T_r^C\left(G'_i(t), G_{mj}(t-1)\right) = \\ & G'_i(t)_{a\sim b\to 0} + G_{mj}(t-1)_{1\sim a|b\sim c\to 0} \end{aligned} \tag{8}$$

where, $G'_i(t) \neq G_{mj}(t-1)$; $G'_i(t) \in \boldsymbol{G}'(t)$ denotes the i^{th} antibody of $\boldsymbol{G}'(t)$; $G_{mj}(t-1) \in \boldsymbol{G}_m(t-1)$ denotes the j^{th} antibody selected from $\boldsymbol{G}_m(t-1)$ randomly; c is the length of antibody alleles; a and b indicate random integers between 1 and c; $a \sim b \to 0$ denotes that the a^{th} to the b^{th} alleles of the antibody equal to zero; $1 \sim a \mid b \sim c \to 0$ denotes that the 1^{th} to the a^{th} alleles and the b^{th} to the c^{th} alleles of the antibody equal to zero; + is logical OR operation.

c) Mutation operator $T_m^C : \boldsymbol{G}'''(t) = T_m^C\left(\boldsymbol{G}''(t)\right)$.

For the binary encoding, each allele of $G''_i(t) \in \boldsymbol{G}''(t)$ is performed the reverse operation with probability p_m.

d) Clone selection operator $T_s^C : \boldsymbol{G}_{non}(t) = T_s^C\left(\boldsymbol{G}'''(t)\right)$.

For any $G^*(t) \in \boldsymbol{G}'''(t)$, if and only if $G^*(t)$ satisfies the following relationship,

$$\begin{aligned} &\exists G'''_i(t) \neq G^*(t)(i = 1, 2, ..., N_c) \in G'''(t): \\ &\forall j \in \{1, 2, ..., m\}\left(E_j\left(G'''_i(t)\right) \leq E_j\left(G^*(t)\right)\right) \\ &\wedge \exists k \in \{1, 2, ..., m\}\left(E_k\left(G'''_i(t)\right) < E_k\left(G^*(t)\right)\right) \end{aligned} \tag{9}$$

then $G^*(t)$ is the non-dominated antibody in the current evaluation algebra, otherwise $G^*(t)$ is the dominated antibody. The clone selection operator is to select out the non-dominated antibodies $\boldsymbol{G}_{non}(t)$ from $\boldsymbol{G}'''(t)$. And the scale of $\boldsymbol{G}_{non}(t)$ is N_{non}.

e) Population regeneration operator T_a^C : $\boldsymbol{G}'_{non}(t) = T_a^C\left(\boldsymbol{G}_{non}(t)\right)$.

If $N_{non} > N$, then select out N antibodies with a lesser degree of constraint violations from $\boldsymbol{G}_{non}(t)$, i.e.,

$$\boldsymbol{G}'_{non}(t) = T_a^C\left(\boldsymbol{G}_{non}(t)\right)$$

and $\boldsymbol{G}'_{non}(t)$ contains N antibodies, otherwise select out N-N_{non} antibodies, i.e.,

$$\boldsymbol{G}_{N-N_{non}}(t) = T_a^C\left(\boldsymbol{G}_{non}(t)\right)$$

and the regeneration antibodies are given by,

$$\boldsymbol{G}'_{non}(t) = \boldsymbol{G}_{N-N_{non}}(t) \cup \boldsymbol{G}_{non}(t))$$

f) Memory education operator T_b^C : $\boldsymbol{G}_m(t) = T_b^C\left(\boldsymbol{G}'_{non}(t)\right)$.

Assume that an antibody of $\boldsymbol{G}'_{non}(t)$ is $G^i_{non}(t)$ and another antibody of memory cells $\boldsymbol{G}_m(t)$ is $G^j_m(t)$. If the degree of constraint violations of $G^i_{non}(t)$ is less than that of $G^j_m(t)$, delete $G^j_m(t)$ and add $G^i_{non}(t)$ into $\boldsymbol{G}_m(t)$. When the degree of constraint violations of each antibody in $\boldsymbol{G}'_{non}(t)$ is greater than or equal to that in $\boldsymbol{G}_m(t)$, the memory education is finished.

4.3 Proposed fault diagnosis process

Based on the above analytic model and the solving approach, the power fault diagnosis process based on the improved immune clonal multi-objective optimization algorithm is as follows:

Step 1: The outage area is identified to obtain the suspected fault section with the network topology determination method [17].

Step 2: Determine the set of fault components (i.e., set $\boldsymbol{D}$) in the fault section and the sets of PRs and CBs corresponding to $\boldsymbol{D}$ (i.e., set $\boldsymbol{R}$ and set $\boldsymbol{C}$).

Step 3: Calculate the actual and the expected states of PRs and CBs (i.e., $r(\boldsymbol{G})$, $c(\boldsymbol{G})$, $r^*(\boldsymbol{G})$, and $c^*(\boldsymbol{G})$).

Step 4: Construct the objective function $E(\boldsymbol{G})$ as shown in Eq. (1) and transform it into $E'(\boldsymbol{G})$ as shown in Eq. (5).

Step 5: Using Eq. (5) as the objective function, an improved immune clonal multi-objective optimization algorithm is applied to solve the optimal solution ($\boldsymbol{D}^*$, $\boldsymbol{R}^*$, $\boldsymbol{C}^*$, $\boldsymbol{F}^*$, $\boldsymbol{M}^*$).

Step 6: ($\boldsymbol{D}^*$, $\boldsymbol{R}^*$, $\boldsymbol{C}^*$, $\boldsymbol{F}^*$, $\boldsymbol{M}^*$) is the optimal FH. And $\boldsymbol{D}^*$ is applied to identify the real fault component; $\boldsymbol{F}^*$ and $\boldsymbol{M}^*$ are used to evaluate the operating states of PRs and CBs.

Step 7: Evaluate the states of the received alarms via Eq. (2).

5. Simulation Analysis

5.1 Fault case 1

5.1.1 Test system

To evaluate the performance of the proposed analytic model-based method, a realistic fault scenario is simulated on a 220kV local power system as shown in Fig. 2.

Table 1 shows the associated alarms obtained from the console in the power dispatching center. Base on the result of the power grid topology analysis [17], the outage area contains 5 suspected fault components including Hedong line B, Helian line B, 220kV Bus II, Hejin line B and Lihe line, denoted by $\boldsymbol{D}$=(d_1, d_2, d_3, d_4, d_5). The associated CBs include CB 6552, 6611, 6013, 6617, 6614, 6600, 6612, 6312 and 6811, denoted by $\boldsymbol{C}$=($c_1, c_2, ..., c_9$). The PRs of d_1 include differential PR, distance PR I, distance PR II and distance PR III in Henan substation and in Dongjiao substation respectively, so do the PRs of d_2 in Henan substation and in Hegang power plant, the PRs of d_4 in Henan substation and in Jinshan substation, and the PRs of d_5 in Henan substation and in Ganshi power plant. The PR of d_2 includes differential PR in Henan substation. CBs, configured failure PR, include CB 6611, CB 6617, CB 6614 and CB 6612. The number of PRs is 37 totally, denoted by $\boldsymbol{R}$=($r_1, r_2, ..., r_{37}$).

PRs associated with received alarms are r_1, r_2, r_5, r_6 and r_{34}, and CBs are c_1, c_3, c_4, c_5, c_6, c_8 and c_9. The observed states corresponding to $\boldsymbol{R}$ and $\boldsymbol{C}$ are $\boldsymbol{R}'$ =($r_1', r_2', ..., r_{37}'$) and $\boldsymbol{C}'$ =($c_1', c_2', ..., c_9'$), where r_1', r_2',

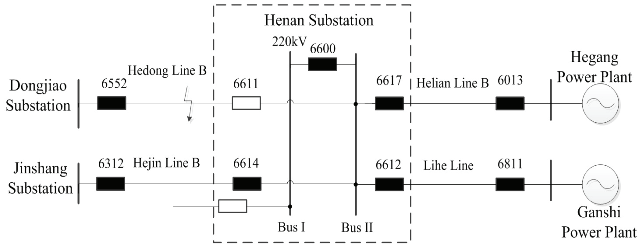

Fig. 2. Electrical connection diagram of a local power grid

Table 1. Fault alarms received by the power dispatching center

Order	Fault occurrence time	Fault alarm description
1	20121130_163401122	Differential PR of Hedong line B in Henan substation operates.
2	20121130_163401122	Distance PR I of Hedong line B in Henan substation operates.
3	20121130_163401122	Differential PR of Hedong line B in Dongjiao substation operates.
4	20121130_163401122	Distance PR I of Hedong line B in Dongjiao substation operates.
5	20121130_163401240	CB 6552 of Dongjiao substation is tripped off.
6	20121130_163401452	Failure startup PR of Hedong line B in Henan substation operates.
7	20121130_163401458	Failure PR of Bus II PR device in Henan substation operates.
8	20121130_163401562	CB 6600 in Henan substation is tripped off.
9	20121130_163401562	CB 6614 in Henan substation is tripped off.
10	20121130_163401562	CB 6617 in Henan substation is tripped off.
11	20121130_163401562	CB 6312 in Jinshan substation is tripped off.
12	20121130_163401562	CB 6811 in Ganshi power plant is tripped off.
13	20121130_163401562	CB 6013 in Hegang power plant is tripped off.

r_5', r_6', r_{34}', c_1', c_3', c_4', c_5', c_6', c_8' and c_9' equal to 1 and the remaining r' and c' equal to 0.

According to the small probability event [13], the relationship of $r_i \in \boldsymbol{R}$ can be given by,

$$\begin{cases} m_{r_i} = 0, & r_i' = 0 \\ f_{r_i} = 0, & r_i' = 1 \end{cases}$$

Similarly, the relationship of $c_i \in \boldsymbol{C}$ can be given by,

$$\begin{cases} m_{c_i} = 0, & c_i' = 0 \\ f_{c_i} = 0, & c_i' = 1 \end{cases}$$

Therefore, the variable values of $\boldsymbol{F}$ and $\boldsymbol{M}$ can be determined, and f_{r_1}, f_{r_2}, f_{r_5}, f_{r_6}, $f_{r_{34}}$, m_{r_3}, m_{r_4}, $m_{r_7} \sim m_{r_{33}}$, $m_{r_{35}}$, $m_{r_{36}}$, $m_{r_{37}}$, f_{c_1}, f_{c_3}, f_{c_4}, f_{c_5}, f_{c_6}, f_{c_8}, f_{c_9}, m_{c_2} and m_{c_7} equal to 0.

Table 2. Comparison of top three optimal solutions

Order	Value of $E(\mathbf{G})$	Feasible solution ($\boldsymbol{D}^*$, $\boldsymbol{R}^*$, $\boldsymbol{C}^*$, $\boldsymbol{F}^*$, $\boldsymbol{M}^*$)
1	1.55	$d_1, r_1, r_2, r_5, r_6, r_{34}, c_1, c_3, c_4, c_5, c_6, c_7, c_8, c_9, f_{c2}$
2	2.05	$d_1, r_1, r_2, r_5, r_6, r_{34}, c_1, c_2, c_3, c_4, c_5, c_6, c_7, c_8, c_9, m_{r34}$
3	3.75	$r_1, r_2, r_5, r_6, r_{34}, c_1, c_3, c_4, c_5, c_6, c_7, c_8, c_9, f_{c2}, m_{r1}, m_{r2}, m_{r5}, m_{r6}$

5.1.2 Fault diagnosis solution and result analysis

According to the above variable associated with the fault scenario, the objective function can be given by,

$$E(\boldsymbol{G}) = 0.55 \times \left[\sum_{i=1}^{37} \left| r_i(\boldsymbol{G}) - r_i^*(\boldsymbol{G}) \right| + \sum_{j=1}^{9} \left| c_j(\boldsymbol{G}) - c_j^*(\boldsymbol{G}) \right| \right] + \left[\sum_{i=1}^{37} \left| r_i' - r_i(\boldsymbol{G}) \right| + \sum_{j=1}^{9} \left| c_j' - c_j(\boldsymbol{G}) \right| \right] \tag{10}$$

$$H(\boldsymbol{G}) = \sum_{i=1}^{37} \left(f_{r_i} m_{r_i} + r_i f_{r_i} + \overline{r}_i m_{r_i} + r_i^* m_{r_i} + \overline{r}_i^* f_{r_i} \right) + \sum_{j=1}^{9} \left(f_{c_j} m_{c_j} + c_j f_{c_j} + \overline{c}_j m_{c_j} + c_j^* m_{c_j} + \overline{c}_j^* f_{c_j} \right) \tag{11}$$

The actual and the expected states of PRs and CBs can be obtained on the basis of the calculation method in [13], and $r^*(\boldsymbol{G})$, $r(\boldsymbol{G})$, $c^*(\boldsymbol{G})$, $c(\boldsymbol{G})$, r' and c' are substituted into Eq. (10) and (11). And then the improved immune clonal multi-objective optimization algorithm is applied to solve $\min\left(E(\boldsymbol{G}), H(\boldsymbol{G})\right)$. Choosing appropriate parameters of the optimization algorithm, the fault component can be located accurately. The method parameters are set as follows: N=100; Max evolution algebra is 500; β=0.8; p_c=0.5; p_m=0.3. The diagnostic results are shown in Table 2, and the variables listed in Table 2 equal to 1.

The solution corresponding to $E(\mathbf{G})$ with equaling to 1.55 can be confirmed as the optimal solution, which fits the realistic fault scenario best. The diagnostic result can be explained that the fault component is Hedong line B, and CB 6611 in Henan substation fails to be tripped off. In addition, comparing $\boldsymbol{R}^*(\boldsymbol{C}^*)$ with $\boldsymbol{R}'$ ($\boldsymbol{C}'$) via Eq. (2), the alarm of CB 6612 in Henan substation can be confirmed as the missing alarm. This fault diagnosis conclusion is consistent with the realistic fault scenario.

5.2 Fault case 2

Fig. 3 shows a typical 4-substation power system

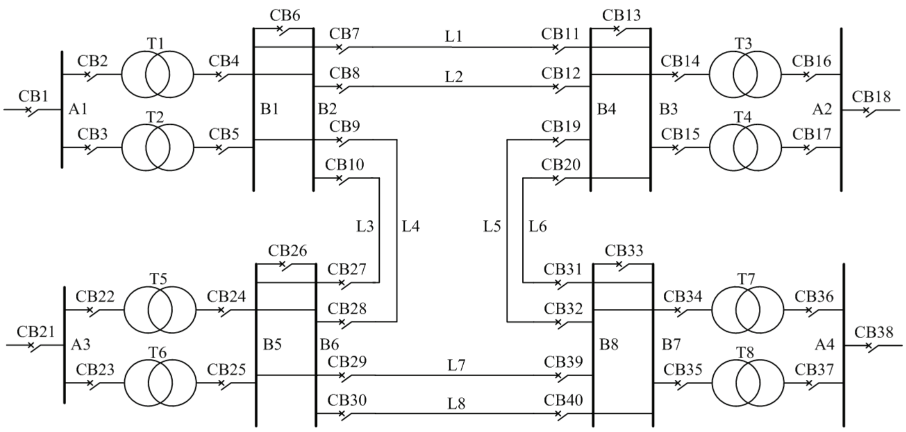

Fig. 3. Typical 4-substation power system

Table 3. Comparison of diagnostic results based on different analytic model-based methods

Scenario	Fault alarm	Diagnostic result In [9]	Diagnostic result In [13]	Diagnostic result In this paper
1	B1m, L2Rs, L3Rs, CB5, CB7, CB9, CB12, CB27	B1	B1	B1
2	B1m, B2m, L1Sm, L1Rm, L1Rp, L2Rm, L2Rp, CB4, CB5, CB6, CB7, CB8, CB9, CB10, CB11, CB12	①B1, B2, L1 ②B1, B2, L1, L2	B1, B2, L1, L2	B1, B2, L1, L2
3	L1Sm, L1Rp, L2Sp, L2Rp, L7Sp, L7Rm, L8Sm, L8Rm CB7, CB8, CB11, CB12, CB29, CB30, CB39, CB40	L1, L2, L7, L8	①L1, L2, L7, L8 ②L1, L7, L8	L1, L2, L7, L8
4	A3m, B6m, CB21, CB22, CB23, CB24, CB25, CB27, CB28, CB29, CB30	A3, B6	A3, B6	A3, B6
5	A3m, T5p, CB21, CB22, CB23, CB26, CB28, CB30	①A3, T5 ②A3, T5, B6	A3, T5	A3,T5
6	T6p, L3Sm, L3Rm, CB10, CB25, CB26, CB29	L3	①L3 ②L3, T6	L3

Note: T, B and L denote a substation, a bus and a line respectively; S and R denote the head and end of the line; m, p and s denote main, local back-up and remote back-up PRs individually consisting of 28 components, 40 CBs and 124 PRs, and the PR configuration information refers to [10, 13]. Several complex fault scenarios with one or more PRs and/or CBs malfunctioning and/or an alarm or alarms of these PRs and/or CBs failing are simulated. Comparison of the diagnostic results based on the developed analytic model-based method and the existing analytic model-based methods in [9] and [13] are shown in Table 3.

As shown in Table 3, the developed analytic model-based method does not have multiple solutions, while the other analytic model-based methods shown in [9] and [13] all have multiple solutions. Through the further analysis of the fault scenarios in Table 3, the diagnostic results of the proposed method are correct and reasonable.

6. Conclusion

This paper presents an improved analytic model for the power system fault diagnosis, which takes into account the interaction between the uncertainty involved with PR operation and CB tripping and the uncertainty of the alarm reception. The proposed model can remove the effect of multiple solutions generated by more malfunctioned PRs and/or CBs and/or missing and/or incorrect alarms.

With transforming constraints into an objective function, the constrained optimization problem is converted to the unconstrained multi-objective optimization problem. This transformation can eliminate the influence of the subjective factor caused by applying the penalty function method.

The improved immune clonal multi-objective optimization algorithm is put forward to solve the power system fault diagnosis problem, and the results of the test cases of the power system fault diagnosis show that the proposed analytic model-based method is feasible and efficient.

Acknowledgements

This work was supported by the "National Natural Science Foundation of China", no. 51377054, and "The Fundamental Research Funds for the Central Universities", no. 2017XS019.

References

[1] Y. S. Ko, "A Study on the Agent (Protective Device)-based Fault Determination and Separation Methodology for Smart Grid Distribution System," *Journal of Electrical Engineering & Technology*, vol. 10, no. 1, pp. 102-108, Jan. 2015.

[2] C. Wattanasakpubal and T. Bunyagul, "Algorithm for Detecting, Identifying, Locating and Experience to Develop the Automate Faults Location in Radial Distribution System," *Journal of Electrical Engineering & Technology*, vol. 5, no. 1, pp. 36-44, Jan. 2010.

[3] C. Fukui and J. Kawakami, "An Expert System for Fault Section Estimation Using Information from Protective Relays and Circuit Breakers," *IEEE Trans. Power Delivery*, vol. 1, no. 4, pp. 83-90, Oct. 1986.

[4] V. N. Ghate and S. V. Dudul, "Induction Machine Fault Detection Using Generalized Feed Forward Neural Network," *Journal of Electrical Engineering & Technology*, vol. 4, no. 3, pp. 389-395, 2009.

[5] G. Mani and J. Jerome, "Intuitionistic Fuzzy Expert System based Fault Diagnosis using Dissolved Gas Analysis for Power Transformer," *Journal of Electrical Engineering & Technology*, vol. 9, no. 6, pp. 2058-2064, Nov. 2014.

[6] X. Luo and M. Kezunovic, "Implementing Fuzzy Reasoning Petri-nets for Fault Section Estimation," *IEEE Trans. Power Delivery*, vol. 23, no. 2, pp. 676-685, Apr. 2008.

[7] X. H. Luo and X. Y. Tong, "Structure-variable Bayesian Network for Power System Fault Diagnosis Considering Credibility," *Power System Technology*, vol. 39, no. 9, pp. 2658-2664, Sep. 2015.

[8] C. L. Hor, P. A. Crossley and S. J. Watson, "Building Knowledge for Substation-based Decision Support Using Rough Sets," *IEEE Trans. Power Delivery*, vol. 22, no. 3, pp. 1372-1379, July 2007.

[9] X. N. Lin, S. H. Ke, Z. T. Li, H. L. Weng and X. H. han, "A Fault Diagnosis Method of Power Systems Based on Improved Objective Function and Genetic Algorithm-Tabu Search," *IEEE Trans. Power Delivery*, vol. 25, no. 3, pp. 1268-1274, July 2010.

[10] F. S. Wen and Z. X. Han, "Fault Section Estimation in Power Systems Using Genetic Algorithm and Simulated Annealing," *Proceedings of the CSEE*, vol. 14, no. 3, pp. 29-35, May 1994.

[11] F. S. Wen and Z. X. Han, "Fault Section Estimation in Power Systems Using a Genetic Algorithm," *Electric Power Systems Research*, vol. 34, no. 3, pp. 165-172, Feb. 1995.

[12] W. X. Guo, F. S. Wen, G. Ledwich, Z. W. Liao, X. Z. He and J. H. Liang, "An Analytic Model for Fault Diagnosis in Power Systems Considering Malfuctions of Protective Relays and Circuit Breakers," *IEEE Trans. Power Delivery*, vol. 25, no. 3, pp. 1393-1401, July 2010.

[13] D. B. Liu, X. P. Gu and H. P. Li, "A Complete Analytic Model for Fault Diagnosis of Power Systems," *Proceedings of the CSEE*, vol. 31, no. 34, pp. 85-93, Dec. 2011.

[14] D. M. Zhao, X. Zhang, J. Wei, W. C. Liang and D. Y. Zhang, "Power Grid Fault Diagnosis Aiming at Reproducing the Fault Process," *Proceedings of the CSEE*, vol. 34, no. 13, pp. 2116-2123, May 2014.

[15] R. H. Shang, L. C. Jiao, C. X. Hu and J. J. Ma, "Modified Immune Clonal Constrained Multi-Objective Optimization Algorithm," *Journal of*

Software, vol. 23, no. 7, pp. 1773-1786, July 2012.
[16] R. H. Shang, L. C. Jiao and W. P. Ma, "Immune Clonal Multi-Objective Optimization Algorithm for Constrained Optimization," *Journal of Software*, vol. 19, no. 11, pp. 2943-2956, Nov. 2008.
[17] M. Prais and A. Bose, "A Topology Processor That Tracks Network Modifications over Time," *IEEE Trans. Power Systems*, vol. 3, no. 2, pp. 992-998, Aug.1988.

Shoupeng Wang He is a Ph.D. candidate in the School of Electrical and Electronic Engineering, North China Electric Power University. He received the B.S. degree in Electrical Engineering and Automation from North China Electric Power University, and his M.S. degree in Electrical Engineering from Xi'an University of Science and Technology. His current interests include analysis, operation and protection of electric power system, and power grid fault diagnosis.

Dongmei Zhao She is a professor and Ph.D. student supervisor of the School of Electrical and Electronic Engineering, North China Electric Power University. She received the B.S. degree in the electric power system and its automation from Wuhan Institute of Hydraulic and Electric Engineering (currently known as Wuhan University), and her M.S. and Ph.D. degree in the electric power system and its automation from North China Electric Power University. Her current interests include analysis, operation and optimization of electric power system, electric power system with new energy sources, applications of artificial intelligence in electric power system.